ISSN: 2689-1204

Research Article

Journal of Applied Material Science & Engineering Research

Fly Ash Derived FAU Zeolite for Desulfurization of Petroleum Feedstocks and Water Purification

Januario Da Costa Hossi[1*], Diakanua Nkazi[1], Josias van der Merwe[1], Atuman Samaila Joel[1] and Kevin Graham Harding[1]

[1]*School of Chemical and Metallurgical Engineering, Faculty of Engineering and Built Environment, University of the Witwatersrand, Johannesburg, South Africa*

[*]Corresponding Author
Januario Da Costa Hossi, School of Chemical and Metallurgical Engineering, Faculty of Engineering and Built Environment, University of the Witwatersrand, Johannesburg, South Africa.

Submitted: 2023, June 25; **Accepted:** 2023, Aug 13; **Published:** 2023, Sep 12

Citation: Hossi, J. D., Nkazi, D., Merwe, J. V., Joel, A. S., Harding, K. G. (2023). Fly Ash Derived FAU Zeolite for Desulfurization of Petroleum Feedstocks and Water Purification. *J App Mat Sci & Engg Res, 7*(2), 129-140.

Abstract

Zeolites are expensive materials which find broad applicability as adsorbents and catalyst for a variety of industrial processes attributed to their structure with specific surface, well defined pore dimension, and chemical properties. The synthesis of zeolites from coal fly ash (CFA) is widely reported and offers an opportunity to valorize waste in such a way that creates great environmental and economic impacts. In this study the alkaline hydrothermal synthesis method was used to identify the key synthesis parameters for fly ash-to-zeolites conversion and what their effects are on physiochemical properties of the resulting zeolite. The raw CFA was obtained from Sasol Coal mining, Mpumalanga, South Africa, and used as source of alumina and silica that gave the zeolite formation. Prior to hydrothermal synthesis, the CFA was calcined at high temperature, fused with sodium hydroxide, dissolved with appropriate volume of deionized water, and exposed to an aging step with stirring for a few hours. The synthesis was optimized by varying the reaction conditions, such as composition of starting materials, synthesis temperature, and time which achieved a faujasite (FAU) zeolite with good crystallinity yield. Treated CFA revealed good properties of Si/Al ratio, surface area, thermal stability, improved morphology, N_2-adsorption, and good cationic exchange capacity characteristic of FAU zeolites. The as-prepared FAU zeolite showed very satisfactory desulfurization capacity, reducing sulfur to less than half of its initial concentration in diesel and gasoline. Thus, the CFA-to-zeolite conversion can gain notice amongst investors due to its potential market value while assisting with solid waste management as practical way to relieve environmental pressures of coal ash dumps to support sustainable development.

1. Introduction

Coal fly ash (CFA) is a by-product from combustion of coal in thermal power plants and is considered as one of the most abundant anthropogenic materials [1]. While the use of coal as source of energy still forms a core part of economic growth in many parts of the world, the management of CFA increasingly becomes important [2]. The enormous amount of CFA generated annually causes large acres of land to be occupied by ash ponds resulting in soil being unavailable to other important sectors such as agriculture [3]. South Africa's power stations generate approximately 40 metric tons of CFA per year but only 5.5% is reported to be utilized in construction industries as cement additive (4). The lack of waste recycling opposes the circularity of resources and becomes the great cause of several environmental problems [3-5]. Creating production-to-consumption systems that are restorative and regenerative could make engineering systems more environmentally benign whilst creating positive economic impacts for sustainable development [6,7].

There is a huge potential of CFA as cheap and effective raw material for synthesis of highly valuable zeolites [3]. The recoverable amounts of SiO_2 and Al_2O_3 in CFA make this material a great precursor of zeolites (8). According to Petrov and Michalev [9], CFA from coal-based power plants contains up to 80 wt. % SiO_2 and Al_2O_3. This may bring the cost of zeolite production to 5 times lower than that of commercially obtained zeolites (10) and breakthrough a large scale application of zeolites constrained by high price of synthesis from chemical reagents [3,11]. Wastes are cheaper resources and utilization of these leads to by-products valorization, which may generate great economic benefits, while reducing the costs associated with managing waste, and enable circular economy.

Zeolites are a group of naturally occurring microporous of hydrated crystalline aluminosilicates which find several industrial applications as molecular sieves, catalysts, and adsorbents [12]. As demonstrated by several researchers, zeolites are candidate materials for gas separation technology, petroleum refining and, including water purification requiring minimal amounts of sorbent [13-15]. Adsorptive desulfurization is a promising

technology which can selectively remove sulfur from petroleum fuels at ambient pressure and room temperature without adsorbing aromatics and olefins present in the fuel [11]. Because CFA can be used as starting material for the synthesis of valuable zeolites, adsorptive desulfurization using zeolites could thus offer an avenue of CFA valorization. There are well-known processes to recover alumina silicates from CFA analogous to the formation of natural zeolites from volcanic deposits; Yoldi et al. [11] reported a few methds of zeolites synthesis from CFA including microwave assisted hydrothermal, alkali-digestion hydrothermal, and molten salt method. Ojha et al. [10] believe that the alkali-fusion method, followed by hydrothermal treatment is the most reliable method for obtaining FAU zeolites Na-X and Na-Y anlogous.

The present work identifies the synthesis conditions that yield the best crystalline structure of FAU zeolite from coal fly ash using hydrothermal alkaline method and assesses this against the removal of metals such as Ca^{2+}, Mg^{2+}, and K^{+} from water and desulfurization of petroleum feedstocks such as gasoline and diesel.

2. Method

2.1 Mechanism

Ojha et al. [10] suggested a mechanism that gives reasonable information on zeolites formation from CFA as presented in equations 1 and 2.

$$NaOH + xAl_2O_3.ySiO_2 \xrightarrow{Fusion} Na_2SiO_2 + Na_2AlO_2 \quad (1)$$

$$NaOH\ (aq) + Na_2Al(OH)_4(aq) + Na_2SiO_3(aq) \xrightarrow{room-temperature} [Na_2(AlO_2)y(SiO_2)z.NaOH.H_2O](gel) \xrightarrow{353-413K} Na_p\left[(AlO_2)_p(SiO_2)_q\right].hH_2O \quad (2)$$

2.2 Materials

CFA, collected from Sasol coal mining, Mpumalanga, South Africa, was used as feedstock for synthesis of FAU zeolite. Electron scanning microscopy (EDS) analysis revealed the as-received CFA comprising 21 wt. % Si, 56 wt. % O_2 and 16.5 wt. % Al_2. The amount of silica and alumina in the CFA confirmed the suitability of using this waste for zeolite production. In addition to CFA, NaOH was used as base, whereas HCl (20 %) was used for acid treatment of CFA before hydrothermal crystallization. Metal salts such as KCl, LiCl, $AgNO_3$, and $CuSO_4$ were used as source of cations for cationic exchange of zeolite.

2.3 Synthesis

The synthesis of FAU zeolite from CFA follows the alkaline hydrothermal method from Ojha et al. [10], Wang et al. [16], Ayele et al. [17], and Eterigho-ikelegbe et al. [18] (Fig 1). The as received CFA was calcined at 850 ºC for 2 hours to remove volatile materials and unburned carbon, followed by acid treatment in 20 % HCl solution (10 ml HCl/g Ash) to dealuminate and remove iron in CFA for activation of aluminosilicate minerals [19]. The acid treated CFA was then mixed with NaOH and fused in a stainless-steel tray at 550 ºC for 2 h and cooled to room temperature. The sample was milled and dissolved with appropriate amounts of deionized water (10g CFA/100 mL), aged for 6 hours with stirring for colloidal formation at room temperature. The resulting gel was then transferred to a Teflon-lined stainless autoclave and kept undisturbed at 100 ºC for 8 hours for hydrothermal crystallization.

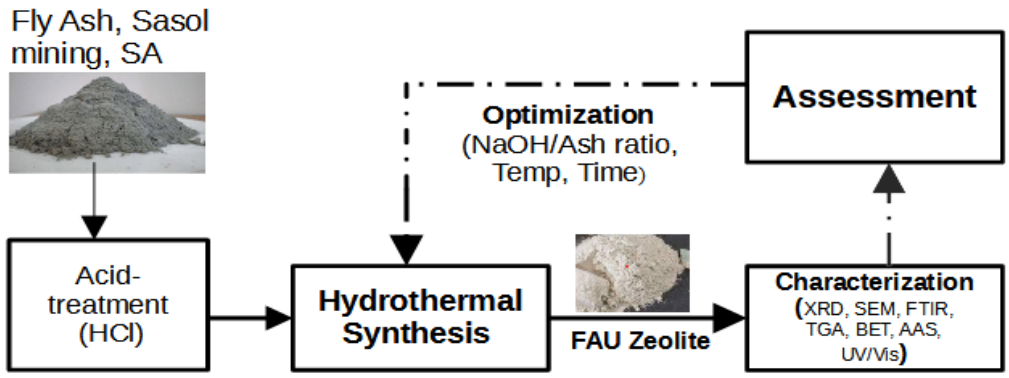

Figure 1: Schematic set-up of zeolite synthesis process

The experiment was repeated with varying NaOH/CFA (wt./wt.) ratios (0.8 to 1.6), synthesis temperature (80 to 120 ºC), and time (6 to 48 h). A portion of as prepared FAU zeolite was ionic exchanged using appropriate alkaline ionic solutions of LiCl and $AgNO_3$ at mild temperature for obtaining Li- and Ag-zeolite, respectively. The resulting solutions were cooled, washed with copious amount of deionized water until pH around 9, filtered, and dried in an oven overnight at 100 ºC. Mixed Li-Ag-zeolite was obtained by further exchanging Li-zeolite in $AgNO_3$ solution using the same cationic exchange procedure above.

2.4 Characterization

The analytical techniques used in this study include X-ray diffraction (XRD), Scanning electron microscopy (SEM), and Energy-dispersive X-ray spectroscopy (EDS) were used to determine the crystallinity, morphology, and composition of the as-prepared zeolite, respectively. The Brunauer-Emmett-Teller (BET) method was used to measure the surface area, pore size and pore volume distribution, and N_2-adsorption isotherms of the crystal and the Fourier-transform infrared (FTIR) was used to analyze the chemical groups present in the as-prepared zeolite thus to test its purity. The absorption spectroscopy (AAS) was used to determine the cationic exchange capacity (CEC). A UV/vis spectrophotometer was used to determine the absorption of desulfurized petroleum feedstocks relative to the absorption of a standard of known sulfur concentration prepared in laboratory.

To determine the crystallinity index of the as-synthesized FAU zeolite, the area of crystalline peaks were divided by the total area of crystalline plus the amorphous peaks of the crystal [19,20]. This was approximated by taking the ratio of the total number of crystalline peaks of the experimental zeolite to the number of crystalline peaks of the reference and multiply by 100 (Eq 3 and 4) [18]. The percent crystallinity was then simply taken as the ratio of the sum of peaks intensity of experimental zeolite to the reference and multiplied by 100 (Eq 5).

$$Crystallinity\ Index = \frac{Area\ of\ Crystalline\ Peaks}{Total\ area\ of\ crystalline\ and\ amorphous\ peaks} \quad (3)$$

$$\%\ Crystallinity = \frac{Crystallinity\ Index\ of\ Experimental\ Zeolite}{Crystallinity\ Index\ of\ Standard} \times 100 \quad (4)$$

$$\%\ Crystallinity = \frac{\sum peaks\ Intensity\ of\ Experimental\ Zeolite}{\sum peaks\ Intensity\ of\ Reference\ Zeolite} \times 100 \quad (5)$$

2.5 Desulfurization Assessment

The adsorptive desulfurization of refined petroleum fuels was achieved by contacting the fuel samples with the fly ash-derived FAU zeolite at batch conditions. The fuel was held inside a vessel to which a known amount of catalyst was added. The reaction mixture was stirred for 3 minutes and kept undisturbed to settle. After an hour, the supernatant, which is the desulfurized fluid, was removed from the solution and analyzed by UV/Vis Spectroscopy (Shimadzu UV-1800 Spectrophotometer) to determine the residual sulfur concentration. The sulfur uptake by FAU zeolite was calculated from the decrease of sulfur concentration in the supernatant solution relative to the initial sulfur concentration in the fuel, or simply by taking the difference in the mass of sulfur in fuel before and after desulfurization per gram of adsorbent (Equation 6).

$$\text{Desulfurization Capacity}\left(\frac{mg}{g}\right) = \frac{Sulfur\ Concentration\ (ppm) \times Fuel\ Volume\ (L)}{Mass\ of\ Adsorbent} \quad (6)$$

2.6 Assessment of Metal Cations Removal From Water

Removal of divalent and monovalent metals such as Ca^{2+}, Mg^{2+}, and K^{+} from water was achieved by contacting the water sample (municipality tape water) with the fly as prepared FAU zeolite in batch conditions. The water was held inside a vessel to which a known amount of FAU zeolite was added. The reaction mixture was stirred for 3 minutes and kept undisturbed to settle. After an hour, the supernatant was removed from the solution and analyzed by Atomic Absorption Spectroscopy (AAS) to determine the demineralization efficiency.

3. Results and Discussion

Raw coal fly ash and the as produced FAU zeolite are illustrated in Photograph 1a and b, respectively.

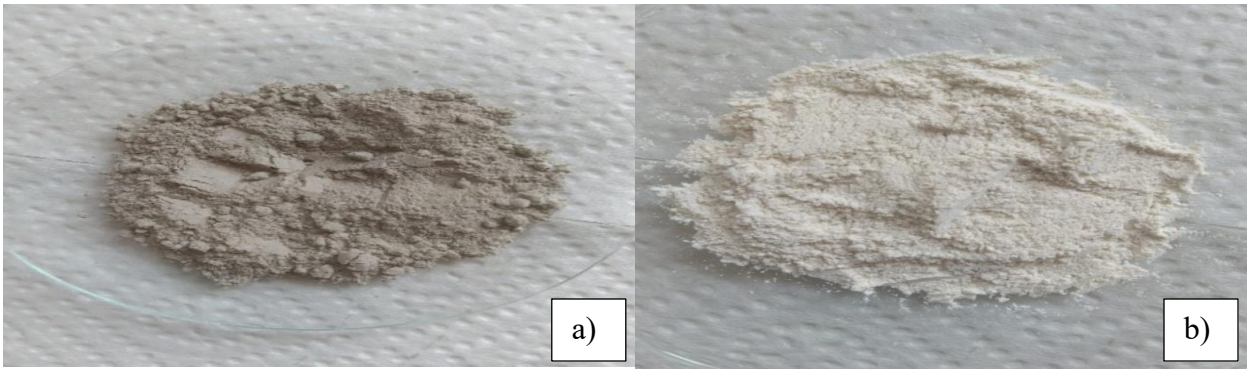

Photograph 1: a) Raw coal fly ash, b) As -produced zeolite

Optical observations of this photograph granted some evidence of the synthesis success before any characterizations were made. Analysis by different analytical tools revealing the physiochemical properties of the produced zeolite as presented below.

3.1 Energy Dispersive X-Ray Spectroscopy Analysis

Energy-dispersive X-ray spectroscopy (EDS) analysis revealed the coal fly ash composition of 21 wt.% Si, 56 wt.% O_2 and 16.5 wt.% Al2. The treated CFA revealed good properties of Si/Al ratio in a range of 1.4-1.6 which falls within law silica FAU-type zeolites family [21]. The raw CFA contained trace mineral elements such as potassium, calcium, titanium, and iron which were absent from the acid treated and crystalized CFA.

3.2 Fourier-Transform Infrared Spectroscopy

The functional groups and molecular bonding of as-produced FAU zeolite were analyzed by Fourier-transform infrared (FTIR) spectroscopy as illustrated in Figure 2.

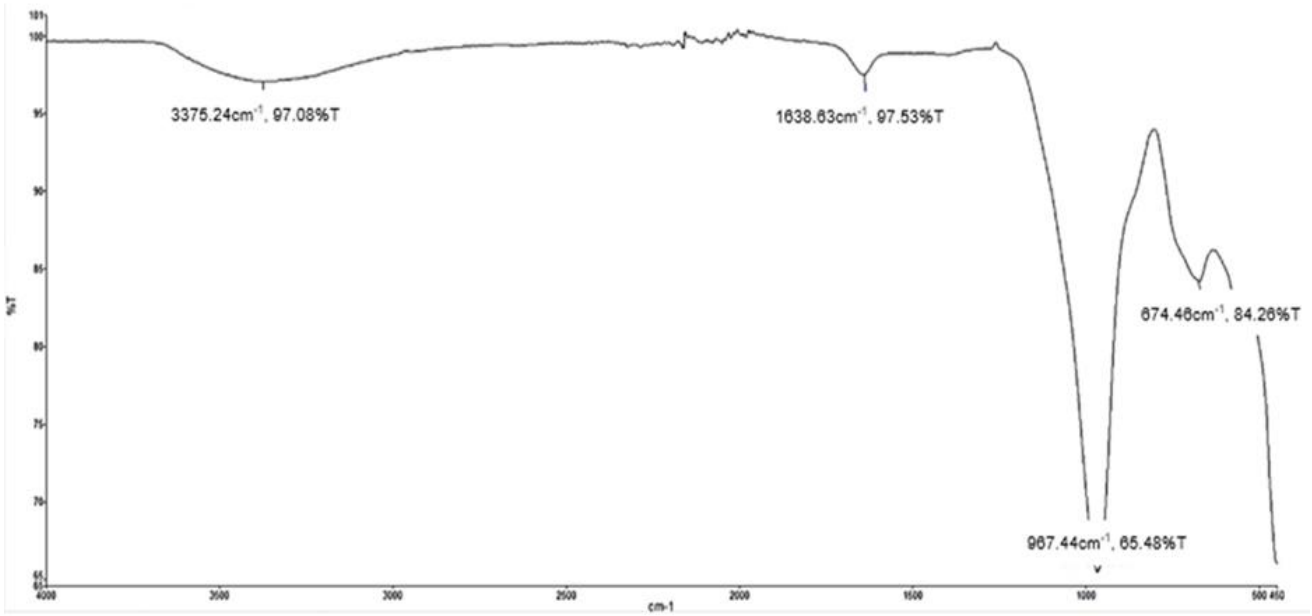

Figure 2: FTIR spectrum of the as-synthesized FAU Zeolite

The FTIR spectrum in Figure 2 reveals no organic chemical groups. This indicates purity of the synthetized FAU zeolite crystals. As reported by Ates [22], the weak peaks that appear over 3376.24 cm^{-1} and 1638 cm^{-1} are characteristic of O-H stretching and bending due to structural and nonstructural adsorbed water molecules; only the peak with the highest intensity (around 9670cm^{-1}) corresponds to vibrations due to the tetrahedral asymmetric linkages. The remaining peaks at 674 cm^{-1} and 84 cm^{-1} indicate the presence of rings linkages in zeolite structure [22].

3.3 Scanning Electron Microscopy Analysis

Analysis by scanning electron microscopy (SEM) reveals the electron micrographs of areas in the mounted samples of the raw CFA and the synthesized FAU zeolites at varying NaOH/Ash ratios. As displayed in Figure 3 (a, b, c, and d), all the images are back scattered electron images (BSE) and acquired at 20 kV.

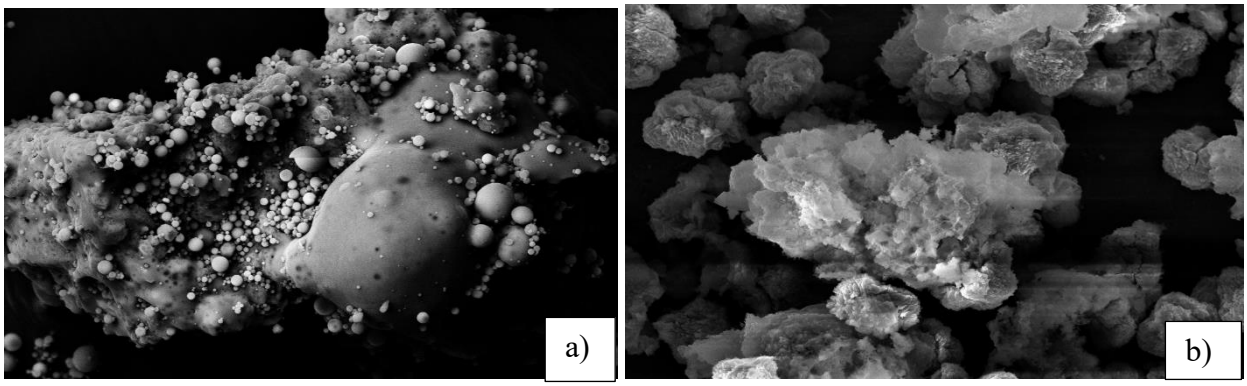

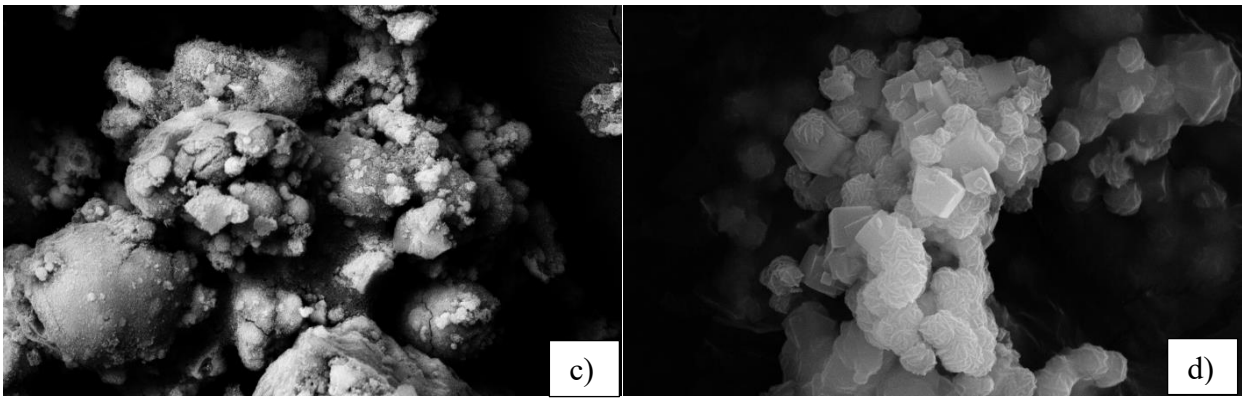

Figure 3: BSE images of a) Raw coal fly ash b), Zeolite at NaOH/Ash 1.2, c) Zeolite at NaOH/Ash 1.4, d) Zeolite at NaOH/ash 1.6

The typical morphology of raw CFA presents abundant spheres associated with coarser and anhedral porous lumps of material as illustrated in Figure 3 (a). In Figure 3 (b and c) some fine angular particles are visible, indicating that zeolite formation has been initiated. These angular particles are better defined in fly ash treated at higher NaOH/Ash ratio of 1.6 (Fig 3d) a product that has clearly resulted in the formation of euhedral (well-formed crystal) aggregates of zeolite crystals.

3.4 X-ray Diffraction Analysis

A conversion method of CFA to zeolite capable of obtaining high crystalline zeolitic structures is necessary to improve the synthesis of zeolites from this waste towards high catalytic performance. In comparing the XRD patterns of the as produced FAU zeolite with the XRD patterns of reference FAU zeolite [23] it is observed that the synthesis was achieved with good crystallinity yield. There is good similarity in the region x-y theta of the as-synthesized zeolite depicted in Figure 8.4 when compared with the reference XRD patterns. Relating the crystalline peaks of the reference zeolite (About 12 peaks) with those generated by the experimental zeolite (10 peaks), using Equation (5), gives a percent crystallinity yield of 83 %. This is a reasonable fit and proves the success of the synthesis route used, although some variations are observed by the peaks position and intensities which could be caused by impurities due to possible sample contamination during synthesis. The XRD of raw CFA and as-prepared FAU zeolite are shown in Figure 4

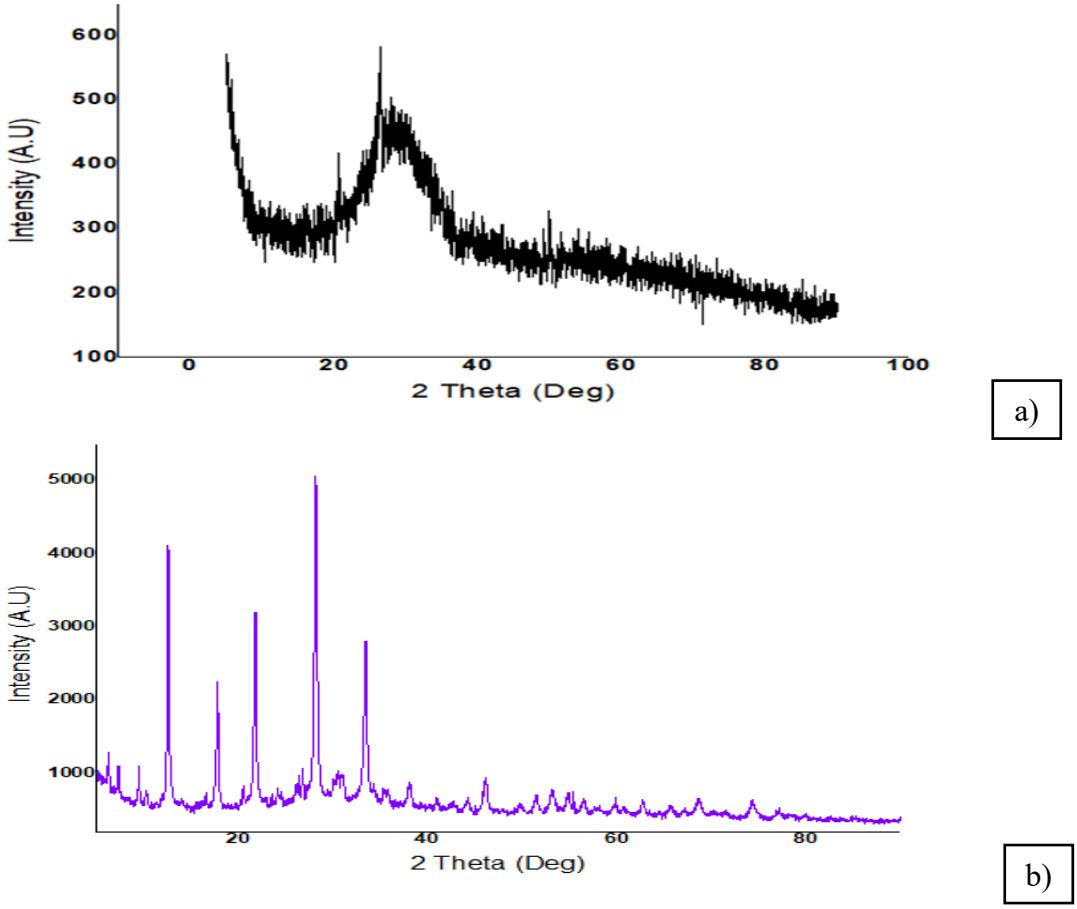

Figure 4: a) X-ray patterns of raw CFA, b) XRD of as-synthesized FAU Zeolite

It is quite uneasy to distinguish FAU zeolite-Y from its zeolite-X analogous. According to Lassinantti [21], zeolite-X and Y are analogous structures of same low silica FAU family but they are slightly differentiated by their Si/Al ratios, 1 to 1.5 and 1.5 to 3, for zeolite-X and zeolite-Y, respectively. Both have high cationic exchange capacity (CEC) which enhances their applicability as sorbents and catalysts [24].

3.4.1 The Effects of Varying the NaOH/ash Ratio on Crystallinity

Figures 5 and 6 depict the effects of varying NaOH/Ash ratios on zeolite crystallinity. The structures obtained at NaOH/Ash ratio below 1.4 are essentially amorphous in nature and not shown here. As the NaOH/Ash was increased from 0.8 to 1.6 the crystallinity yields increased while the proportion of amorphous glass decreased. The intensity of crystalline peaks was intensified at the NaOH/Ash ratio of 1.4. At the NaOH/Ash ratio of 1.6 the peak intensities increased even further as the amorphous content virtually disappeared (Fig 6). This indicates that CFA-to-FAU zeolite conversion occurs optimally between NaOH/Ash ratios of 1.4 and 1.6.

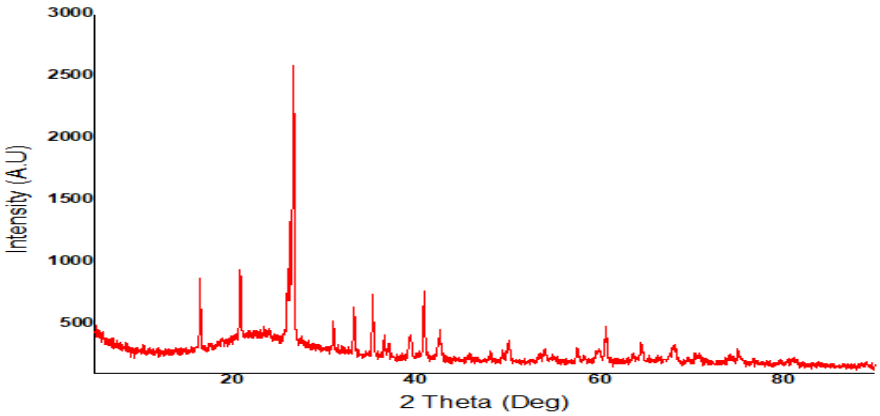

Figure 5: XRD of zeolite formed at NaOH/ash 1.4.

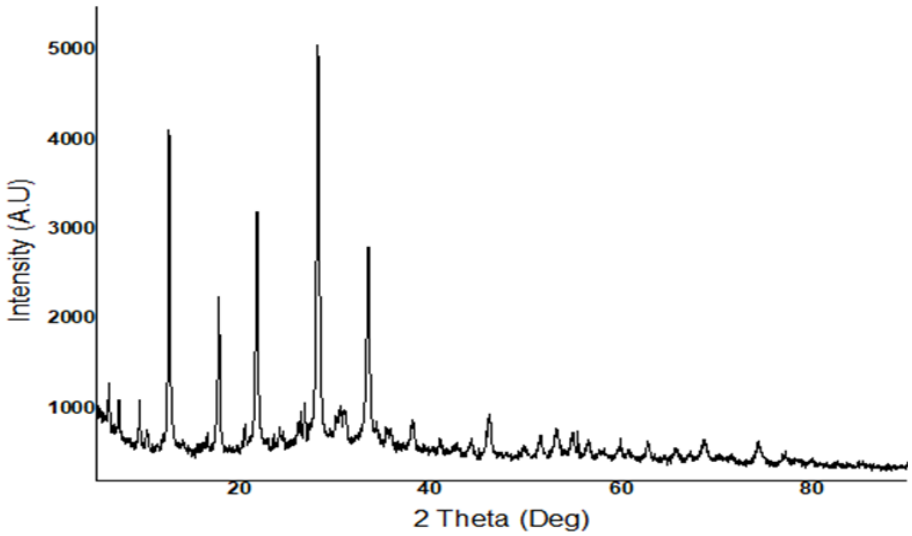

Figure 6: XRD of zeolite formed at NaOH/ash 1.6.

The diffratograms of zeolite sinthesized at NaOH/Ash ratios below 1.4 are not shown since these samples were poorly crystalline indicating that NaOH/Ash ratios below 1.4 are not optimal for CFA-to-FAU zeolite conversion.

3.4.2 The Effects of Synthesis Temperature on Crystallinity

Varying the synthesis temperature from 100 ºC to120 ºC did not convey significant structural changes. Altough not clearly visible from the diffractograms in Figures 8 and 9, the crystalliity obtained at 120 ºC (Fig 7) was slightly higher when compared with that of 100 ºC (Fig 9).

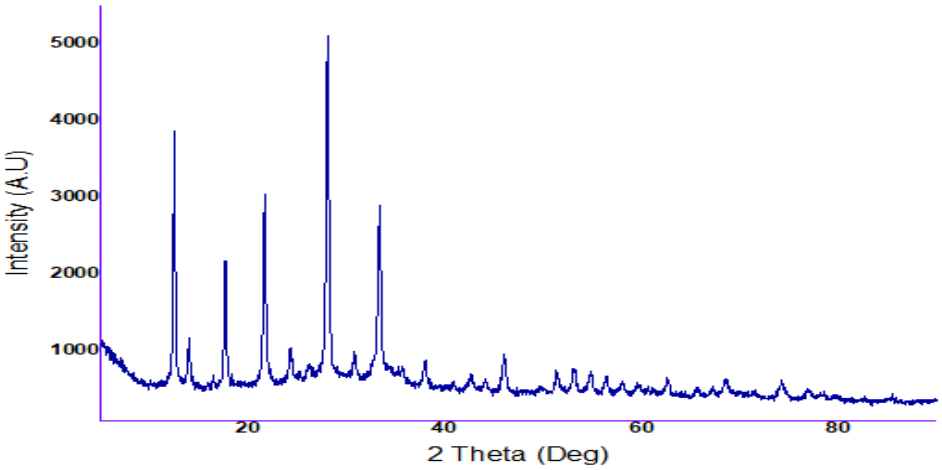

Figure 7: XRD Pattern at Synthesis Temperature (100 ºC)

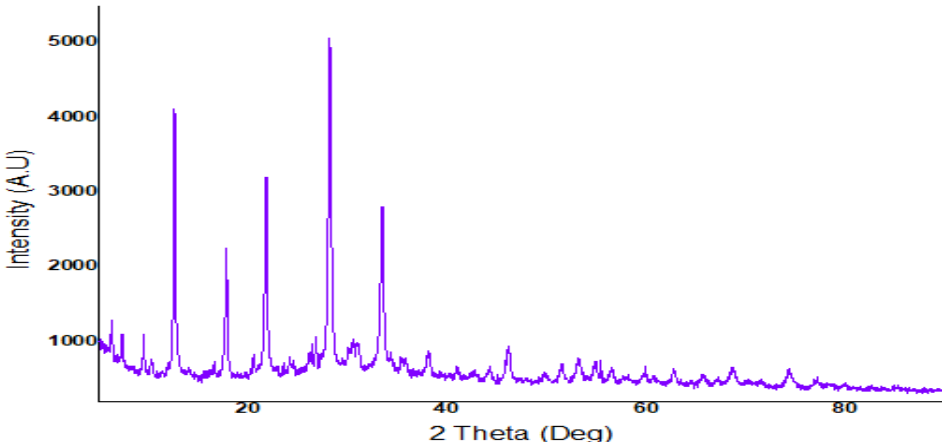

Figure 8: XRD Pattern at Synthesis Temperature (120 ºC)

The diffratograms of zeolite sinthesized below 100 ºC are not shown since these samples were poorly crystalline indicating that the temperatures below 100 ºC are not optimal for zeolite synthesis. Increasing the temperature above 120 ºC during hydrothermal synhtesis would be unecessary waste of energy since this would not improve the crystalinity but lead to formation of other zeoites tyeps such as Sodalite instead of FAU zeolite [25].

3.4.3 Effects of Synthesis Time on Crystallinity

As observed in Figure 9, the synthesis time below 12 hours (black trace) did not generate a well-defined and intense peak of crystalline structure when compared with the structure obtained at 24 hours (blue trace).

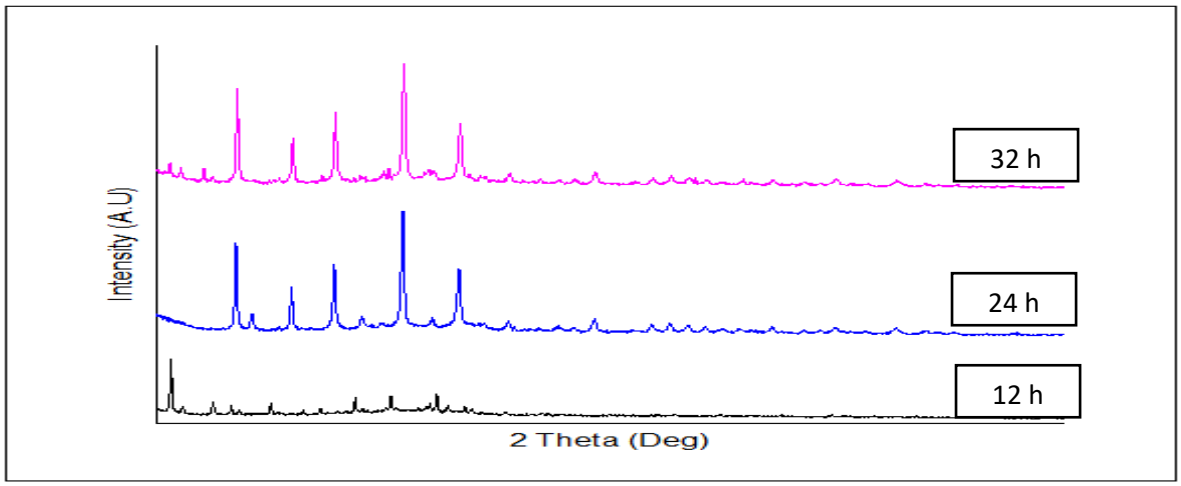

Figure 9: XRD Patterns of the as prepared FAU zeolite at varying synthesis time

Since there are no major structural improvements above 24 hours synthesis, there is no benefit in increasing the synthesis time, the shorter time would also avoid energy penalties.

3.5 Brunauer-Emmett-Teller (BET) analysis

Physical properties of zeolites, such as specific surface area, pore size, and pore volume distribution, are important factors in various zeolite applications. The BET measurements of the as prepared FAU zeolite, including the cationic exchanged forms, are presented in Table 1 and Figure 10.

Sample	BET (m2/g)	Pore Width (nm)	Pore Vol. (cm3/g)	Particle Size (nm)
Starting Zeolite	60.54	1.04	0.07	99.73
Ag-Zeolite	64.00	1.05	0.09	93.73
Li-Zeolite	121.98	0.52	0.10	49.20
LiAg -Zeolite	154.33	0.53	0.26	38.90

Table 1: Surface areas and pore structure measurement by BET

The trend displayed in Table 1 was expected; the surface area usually increases with decreasing particle size and pore diameter. Ag-exchanged zeolite shows BET profile remained closer to that of the starting zeolite, the BET surface areas of other cationic-exchanged zeolites increased significantly from around 60 m^2g^{-1} in the starting zeolite to 154.33 m^2g^{-1} after modifications by cationic exchange. At the same time, the pore widths decreased somewhat from 1 nm in the starting zeolite to near 0.5 nm. According to Murphy [26] large surface areas are beneficial for adsorption as these increase the sorbent loading capacity. Murphy [26] reported pore diameters of 0.5 nm as being effective for molecular sieving. Thus, Li-exchanged zeolite, having 5 Å pore diameter, offers a microporous nature capable of separating N_2 from O_2 in the air based on their kinetic dimeters of 2.90 and 3.14 Å, respectively [27,28]. This could possibly be the reason why Li-exchanged zeolites have been recommend for air separation [29]. LiAg-Zeolite, however, has the largest surface area (154.3 m^2g^{-1}) when compared with Li-exchanged zeolite (121.98 m^2g^{-1}). This gives an evidence to why Epiepang et al. [30] observed a considerable N_2-adsorption improvement when mixed cations zeolite, such as LiAg-zeolite, was used as sorbent for air separation. Mixed cations exchanged zeolites also increase the electrostatic interactions between the adsorbent and the adsorbate which enhances the catalytic activity in addition to size-exclusion mechanism [30].

All isotherms in Figure 10 (a, b, c, and d) show some hysteresis consistent with micropores. As presented in section 3.3, cationic exchange increased the zeolitic surface area while the pores sizes decreased. Cationic exchange also increases the zeolite acidity [27] which improves adsorption. Hence, exclusion by molecular size is not the only separation parameter considered in adsorption. In fact, N_2 has stronger electrostatic interaction with FAU zeolite than O_2 which makes separation of these two molecules much easier [31,32].

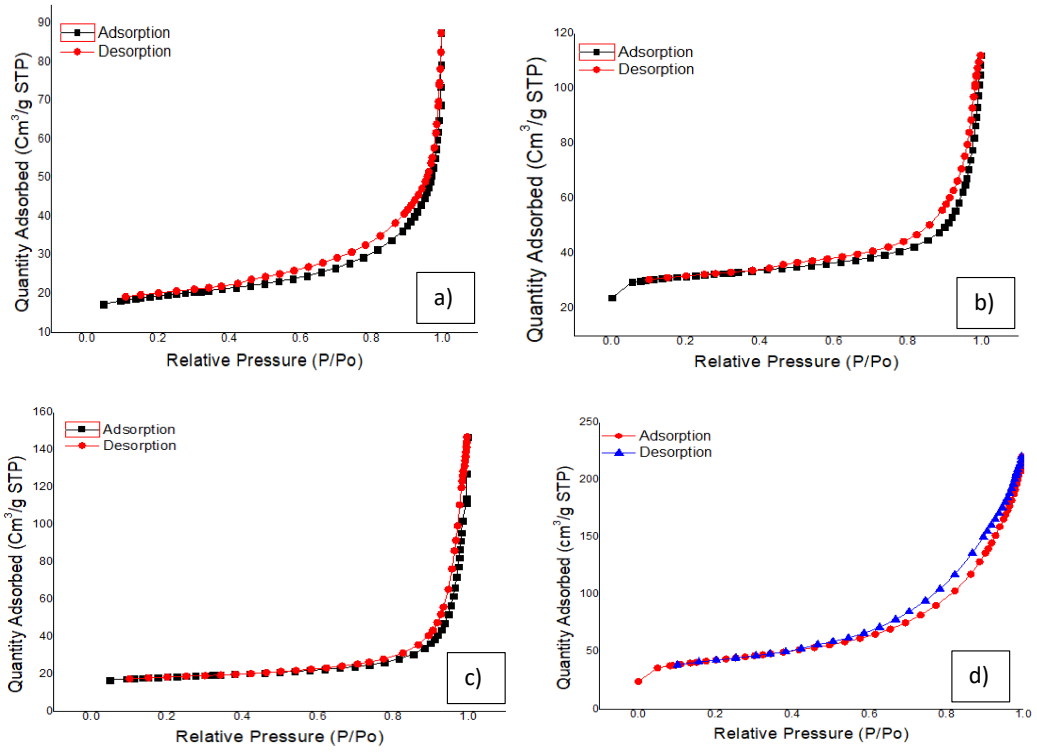

Figure 10: N_2–Adsorption of a) Starting zeolite b) Li – zeolite c) Ag – Zeolite c) d) LiAg – zeolite

The cations on exchanged zeolites improved the zeolite adsorption performance while lowering the amount of sorbent required to elicit an effect [30]. This is observed in Figure 10 (d) which shows a different adsorption pattern when compared to the isotherms in Figure 10 (a, b, and c). Addition of merely minute amounts of silver to a previously lithium-exchanged zeolite enhanced the adsorptive properties of a singly lithium-exchanged zeolite as supported by Sebastian [33]. Based on the results displayed, high aluminium, low silica, and cation-exchanged FAU zeolite gives the best zeolite architecture for N_2-adsorption separation.

3.6 Thermogravimetric Analysis

The thermogravimetric analysis (TGA) proved to be a fast and consistent method to determine the thermal stability of the as-synthesized FAU zeolite.

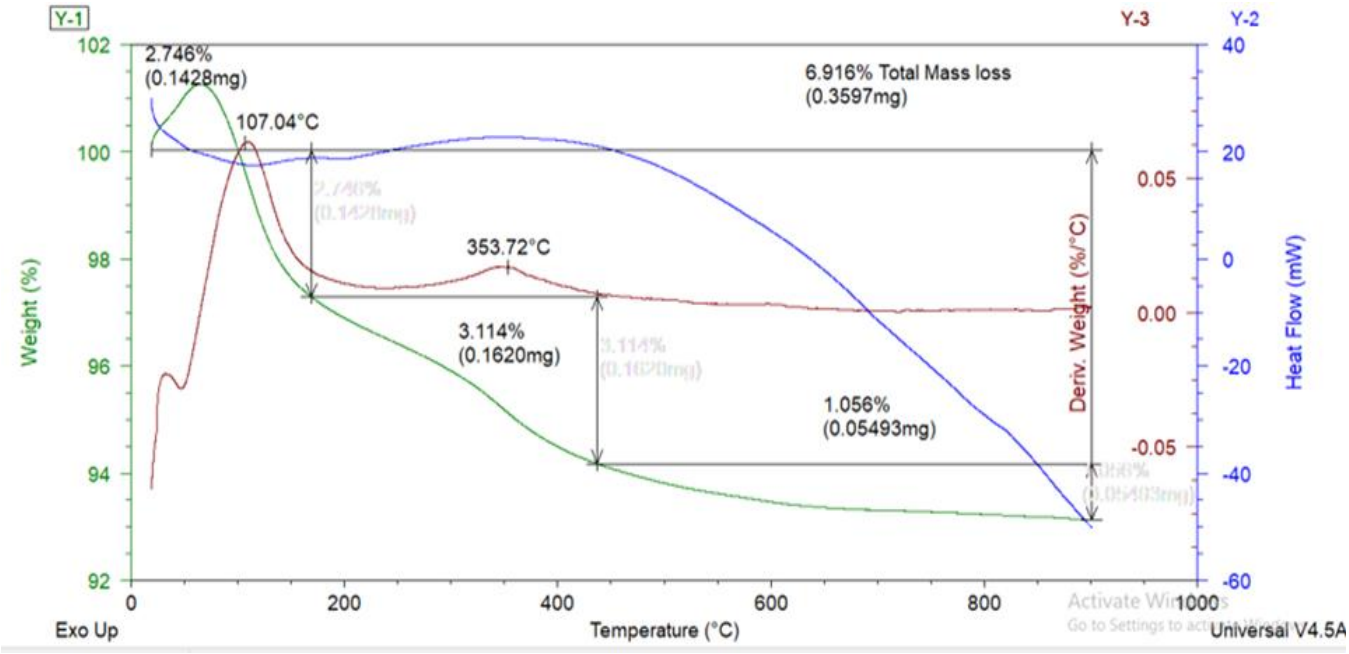

Figure 11: TGA Analysis of Experimental FAU Zeolite (100ºC -900 ºC)

As illustrated in Figure 11, FAU zeolite exhibits a total mass loss (green trace) of 6.9% after heat treated to 600 ºC from around 100 ºC. The mass loss is due to nonstructural water evaporation [34] which did not affect the structural arrangement of the crystalline; the sorbent still retained its catalytic activity after heat treatment. The zeolitic thermal resistance is an outstanding physical property that enhances its application in catalysis in addition to its wide use for production of construction materials [35]. It is exactly this attribute that makes zeolite a choice material for catalysis in harsh environments such as in extreme temperatures of internal combustion engines.

3.7 Removal of Divalent And Monovalent Metals From Water

Atomic Absorption Spectroscopy (AAS), which relates the light absorbed with the concentration of an element, was the fastest method to determine the cationic exchange capacity (CEC) of the as-produced FAU zeolite to assess its effectiveness on removal of metal cations from water. The CEC value of 3.5 MEQ/g zeolite was obtained by taking the difference of the total concentrations of cations in each volume of sample water before and after contacting with the zeolite adsorbent as summarised in Table 2.

Cation	Sample mg/L	Control mg/L	Diff. mg/L	0.1 L
Mg+	3.1	0.3	2.8	0.3
K+	22.4	0.4	22.0	2.2
Ca+	10.8	0.8	10.0	1.0
CEC (MEQ/g Zeolite)				3.5

Table 2: CEC Analysis by AAS

Table 2 shows a significant reduction in the concentration of metal cations in demineralized water. This is very satisfactory because the removal of trace heavy metal cations, such as Cd^{2+}, Pb^{2+}, and Zn^{2+} from wastewater is critical for water purification [15]. The high CEC displayed by the as-produced FAU zeolite on divalent Ca^{2+}, Mg^{2+}, and monovalent K^{+} cations is evidence that the material could be used for removal of monovalent and divalent metal cations from wastewater effluents.

3.8 Desulfurization of Gasoline And Diesel

The performance of the as-prepared FAU zeolite on removal of sulfur in gasoline and diesel was determined by UV/Vis spectroscopy measurements of the original and desulfurized fuel samples.

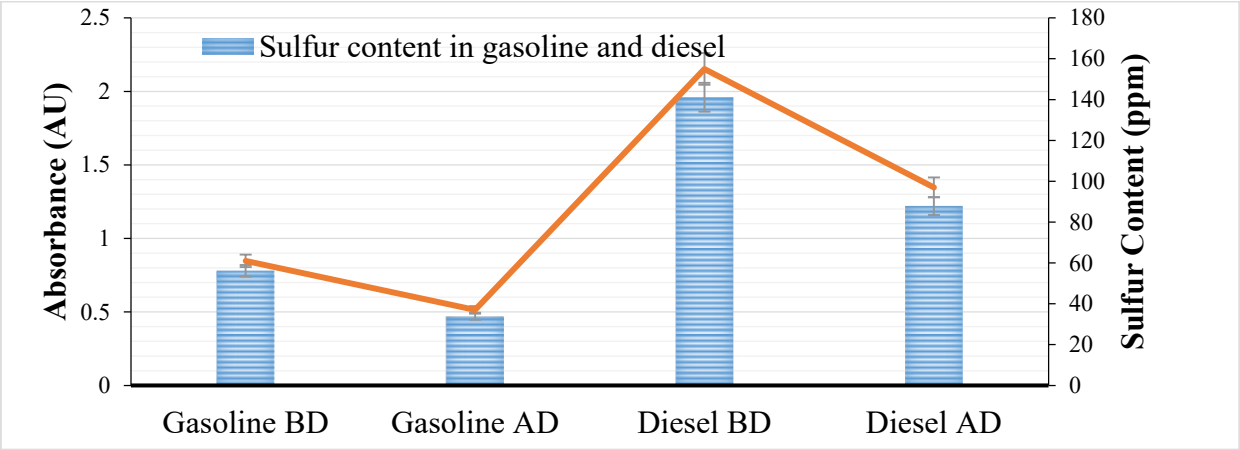

AD* after desulfurization, BD* before desulfurization

Figure 12: Performance of FAU zeolite on gasoline and diesel desulfurization

There was a considerable drop of sulfur concentration from 270 ppm in the non-desulfurized diesel sample to less than 100 ppm after desulfurization (Fig 12). Before desulfurization, gasoline had a sulfur content of approximately 61 ppm, which was reduced to 37 ppm. Thus, halving sulfur levels gasoline and diesel and achieving this at ambient pressure and room temperature could make adsorptive desulfurization very economic with fly ash zeolite as catalyst.

3.9 Cost-benefit Analysis

Production of zeolites from waste resources such as CFA is economically attractive and may overcome the high cost of synthesis from chemical reagents such as silicate and aluminate [9-11]. The recoverable amounts of SiO_2 and Al_2O_3 in CFA make this material a great precursor of zeolites with catalytic activity similar to commercial zeolites [8,16]. Table 3 estimates the cost of preparation of zeolites from CFA at batch scale.

Description	Unit	Quantity	Cost $ USD
Commercial Zeolite	g	1000	1160
Subtotal			**1160**
Experimental Zeolite			
NaOH	g	1600	128
Water	L	100	0.2
Energy	KWh	29	2
Subtotal			**130**
Gross Margin			1029

Table 3: Cost-benefit analysis of production of CFA versus commercial zeolite

Table 3 gives an estimate of daily household energy use which is assumed to cover the daily energy requirements of producing 1 Kg of CFA zeolite. The total daily energy cost of $ USD 2 was obtained by multiplying the price energy of $ USD 0.07 [36] per kWh times 29 kWh per day. The cost of reagents such as NaOH could be obtained at suppliers' website such as Sigma Aldrich. The synthesis at 24 hours gave satisfactory crystallinity yield of the as-produced zeolite, therefore, the energy cost of producing 1 kg zeolite gives reasonable estimate. The amount of water used for hydrothermal synthesis and washing was recorded during experiments and was considered in cost estimation. The water price was obtained from local municipality government websites. This analysis shows that reducing the gross margin to half of the current value due to additional costs such as equipment and labour would keep the cost of zeolites production 5 times lower than commercial zeolites.

Conclusions

The fly ash-to-zeolite conversion has potential to offer an inexpensive alternative to current synthetic zeolites production from chemicals. Many optimization methods have been investigated for hydrothermal synthesis of zeolites from coal fly ash and the combination of these offers the best synthesis zone achieved in this study. The temperature ranging from 100

ºC to 120 ºC, over 24 hours synthesis time, offered the optimal conditions for zeolite conversion, and the NaOH/Ash ratio of 1.6 gave the best crystallinity yield. The composition of the synthesis mixture with respect to the NaOH/Ash ratio, the temperature, and duration of the synthesis were the most important parameters determining the crystallinity and significantly enhanced the morphology of the crystal. The surface area increased by 45.3m2g-1 on average after cationic exchanging with selected metal cations while the pore sizes halved to 0.5 nm from 1 nm. Zeolitic adsorptive desulfurization successfully achieved the removal of sulfur from 270 ppm to less than 100 ppm and from 61 ppm to 37 ppm in diesel and gasoline samples, respectively, at stopped flow and ambient conditions. Treated fly ash is therefore a promising alternative to the refiners' hydrotreatment methods expected to improve the environmental performance of fossil fuels. The physiochemical properties of the as produced FAU zeolite, such as the high cationic exchange capacity, N_2-adsorption, and chemical resistance, grant this material broad industrial applicability in catalysis, gas and liquid separation, and water purification. As zeolites continue fueling their market growth, making the pursuit of methods of efficient production and scalability becomes a subject of practical interest.

Acknowledgement

The authors wish to acknowledge the Ministry of Petroleum and Mineral Resources of Angola for financial lift to this work without which it would be impossible to achieve these goals.

References

1. Zhu, M. H., Kumakiri, I., Feng, Z. J., Hua, X. M., Xia, S. L., Hu, N., ... & Kita, H. (2014). Structure directing agent-free synthesis of ZSM-5 zeolite membranes using coal fly ash as alumina source. Chemistry letters, 43(6), 772-774.
2. Du Plessis, P. W., Ojumu, T. V., Fatoba, O. O., Akinyeye, R. O., & Petrik, L. F. (2014). Distributional fate of elements during the synthesis of zeolites from South African coal fly ash. Materials, 7(4), 3305-3318.
3. Chen, J., & Lu, X. (2018). Synthesis and characterization of zeolites NaA and NaX from coal gangue. Journal of Material Cycles and Waste Management, 20, 489-495.
4. Ndlovu, N. Z., Ameh, A. E., Petrik, L. F., & Ojumu, T. V. (2023). Synthesis and characterisation of pure phase ZSM-5 and sodalite zeolites from coal fly ash. Materials Today Communications, 34, 105436.
5. Keijer, T., Bakker, V., & Slootweg, J. C. (2019). Circular chemistry to enable a circular economy. Nature chemistry, 11(3), 190-195.
6. Chen, T. L., Kim, H., Pan, S. Y., Tseng, P. C., Lin, Y. P., & Chiang, P. C. (2020). Implementation of green chemistry principles in circular economy system towards sustainable development goals: Challenges and perspectives. Science of the Total Environment, 716, 136998.
7. Avraamidou, S., Baratsas, S. G., Tian, Y., & Pistikopoulos, E. N. (2020). Circular Economy-A challenge and an opportunity for Process Systems Engineering. Computers & Chemical Engineering, 133, 106629.
8. Majchrzak-Kucęba, I. (2013). A simple thermogravimetric method for the evaluation of the degree of fly ash conversion into zeolite material. Journal of Porous Materials, 20, 407-415.
9. Petrov, I., & Michalev, T. (2012). Synthesis of zeolite A: a review. Научни трудове на русенския университет, 51, 30-35.
10. Ojha, K., Pradhan, N. C., & Samanta, A. N. (2004). Zeolite from fly ash: synthesis and characterization. Bulletin of Materials Science, 27, 555-564.
11. Yoldi, M., Fuentes-Ordoñez, E. G., Korili, S. A, Gil, A. (2019) Zeolite synthesis from industrial wastes. Microporous Mesoporous Mater;287(March):183–91.
12. Von-Kiti, E. (2017). Synthesis and characterization of zeolites from bauxite and kaolin: application to the removal of heavy metals from mining wastewater (Doctoral dissertation).
13. Siriwardane, R. V., Shen, M. S., & Fisher, E. P. (2003). Adsorption of CO_2, N_2, and O_2 on Natural Zeolites. Energy & fuels, 17(3), 571-576.
14. Hamed, H. H. (2015). Oxygen and nitrogen separation from air using zeolite type 5A. Al-Qadisiyah Journal for Engineering Sciences, 8(2), 147-158.
15. Minceva, M., Fajgar, R., Markovska, L., & Meshko, V. (2008). Comparative study of Zn^{2+}, Cd^{2+}, and Pb^{2+} removal from water solution using natural clinoptilolitic zeolite and commercial granulated activated carbon. Equilibrium of adsorption. Separation Science and Technology, 43(8), 2117-2143.
16. Chunfeng, W., Jiansheng, L. I., Xia, S. U. N., Lianjun, W. A. N. G., & Xiuyun, S. U. N. (2009). Evaluation of zeolites synthesized from fly ash as potential adsorbents for wastewater containing heavy metals. Journal of environmental sciences, 21(1), 127-136.
17. Ayele, L., Pérez-Pariente, J., Chebude, Y., & Díaz, I. (2016). Conventional versus alkali fusion synthesis of zeolite A from low grade kaolin. Applied Clay Science, 132, 485-490.
18. Eterigho-Ikelegbe, O., Bada, S., Daramola, M. O., & Falcon, R. (2021). Synthesis of high purity hydroxy sodalite nanoparticles via pore-plugging hydrothermal method for inorganic membrane development: Effect of synthesis variables on crystallinity, crystal size and morphology. Materials Today: Proceedings, 38, 675-681.
19. Liu, H. (2022). Conversion of harmful fly ash residue to zeolites: innovative processes focusing on maximum activation, extraction, and utilization of aluminosilicate. ACS omega, 7(23), 20347-20356.
20. Liu, B., Sun, H., Peng, T., & He, Q. (2018). One-step synthesis of hydroxysodalite using natural bentonite at moderate temperatures. Minerals, 8(11), 521.
21. Lassinantti, M. (2011). Licentiate Theses. The Jurist: Studies in Church Law and Ministry, 71(2), 480–482.
22. Ates, A. (2019). The modification of aluminium content of natural zeolites with different composition. Powder Technology, 344, 199-207.
23. Vallace, A., Kester, G., Casteel, W., Lau, G., Whitley, R., & Coe, C. (2021). A Study of Structural Defects in X-and Y-Type Zeolites and Their Effect on Their Transformation to Aluminum-Rich Chabazite. The Journal of Physical Chemistry C, 125(23), 12848-12856.
24. Powroznik, K. D. M. C. A. (2018). Natural and synthetic zeolites. synthesis of zeolite X. 1–39.

25. Ruen-ngam, D., Rungsuk, D., Apiratikul, R., & Pavasant, P. (2009). Zeolite formation from coal fly ash and its adsorption potential. Journal of the Air & Waste Management Association, 59(10), 1140-1147.
26. Murphy, K. (2021). Graham's Law Explained: The Difference between Effusion and Permeation. Air Products and Chemicals Inc, 16, 3-5.
27. Freude, D. (2004). Size, Mass and Kinetics of Molecules. Molecular Physics, Chapter Size, October, 1–19.
28. Rege, S. U., & Yang, R. T. (1997). Limits for air separation by adsorption with LiX zeolite. Industrial & engineering chemistry research, 36(12), 5358-5365.
29. Hutson, N. D., Zajic, S. C., & Yang, R. T. (2000). Influence of residual water on the adsorption of atmospheric gases in Li− X zeolite: experiment and simulation. Industrial & Engineering Chemistry Research, 39(6), 1775-1780.
30. Epiepang, F. E., Yang, X., Li, J., Liu, Y., & Yang, R. T. (2018). Mixed-cation LiCa-LSX zeolite with minimum lithium for air separation. AIChE Journal, 64(2), 406-415.
31. Fu, Y., Liu, Y., Yang, X., Li, Z., Jiang, L., Zhang, C., ... & Yang, R. T. (2019). Thermodynamic analysis of molecular simulations of N_2 and O_2 adsorption on zeolites under plateau special conditions. Applied Surface Science, 480, 868-875.
32. Fu, Y., Liu, Y., Li, Z., Zhang, Q., Yang, X., Zhao, C., ... & Yang, R. T. (2020). Insights into adsorption separation of N_2/O_2 mixture on FAU zeolites under plateau special conditions: A molecular simulation study. Separation and Purification Technology, 251, 117405.
33. Sebastian, J. (2011). Adsorption, Catalytic and Photocatalytic Properties of Metal Ion Exchanged Zeolites (Doctoral dissertation).
34. Castro, P. R. D. S. D., Maia, A. Á. B., & Angélica, R. S. (2020). Study of the thermal stability of faujasite zeolite synthesized from kaolin waste from the Amazon. Materials Research, 22.
35. Madzivire, G., Petrik, L. F., Gitari, W. M., Ojumu, T. V., & Balfour, G. (2010). Application of coal fly ash to circumneutral mine waters for the removal of sulphates as gypsum and ettringite. Minerals Engineering, 23(3), 252-257.
36. Department of Minerals Resources and Energy. Electricity Pricing Policy Review Date : February 2022. Gov Not. 2022;(45899):3–123.